Asian Journal of Water, Environment and Pollution. 2026;23(2):025370288.
doi: 10.36922/AJWEP025370288

ORIGINAL RESEARCH ARTICLE

Synthesis of lanthanum oxide/Zeolite Socony Mobil-5 composite and its catalytic activity in formaldehyde degradation

Qingguo Ma*, Sai Yuan, Ye Yuan, Jun Zhong, Ran Wang, Yujie Gong, and Qin Gao

Department of Chemistry and Chemical Engineering, Taiyuan Institute of Technology, Taiyuan, Shanxi, China
***Corresponding author:** Qingguo Ma (maqg@tit.edu.cn)

Received: September 8, 2025; Revised: November 3, 2025; Accepted: November 7, 2025; Published online: November 27, 2025

Abstract: Formaldehyde reacts with proteins, causing their denaturation and exhibiting high toxicity, carcinogenicity, and teratogenicity. In this study, lanthanum (La) oxide (La_2O_3)/zeolite Socony Mobil-5 (ZSM-5) catalyst was synthesized using the equal-volume impregnation method, and formaldehyde in wastewater was efficiently degraded using this catalyst and hydrogen peroxide (H_2O_2) as the oxidant. Based on thermogravimetric analysis of La_2O_3/ZSM-5, ZSM-5, and La (III) nitrate hexahydrate, the optimal calcination temperature of the La_2O_3/ZSM-5 precursor was determined to be 600°C. X-ray powder diffraction and transmission electron microscopy analyses revealed that La_2O_3 was well dispersed on ZSM-5. The effects of La_2O_3 loading, catalyst dosage, H_2O_2 concentration, initial formaldehyde concentration, and solution pH on the degradation rate were systematically investigated. The catalyst exhibited dual functionality, enabling both adsorption and activation of formaldehyde and H_2O_2 molecules. Under optimized conditions—10 wt% La_2O_3, 50 mg/mL catalyst dosage, a molar ratio of H_2O_2 to formaldehyde of 3, pH 5–11, and a reaction time of 20 min—the degradation rate of formaldehyde exceeded 95%. This technique can effectively treat formaldehyde concentrations up to 1.497 mg/mL. This finding offers guidance for designing efficient catalysts applicable to non-Fenton oxidation processes for formaldehyde degradation.

Keywords: Formaldehyde; Lanthanum oxide; Zeolite Socony Mobil-5; Degradation

1. Introduction

Approximately 99% of engineered wood panels are bonded with adhesives such as urea–formaldehyde, melamine–urea–formaldehyde, or phenol–formaldehyde resins.[1] These adhesives are synthesized using formaldehyde as a raw material, thereby generating formaldehyde-containing wastewater. In addition, formaldehyde is widely used as a tanning agent in leather processing, textiles, and other industries.[2] Due to its ability to bind with proteins, formaldehyde exhibits high toxicity along with significant carcinogenic and teratogenic properties. It not only poses severe risks to human health but also contributes to environmental pollution.

Current formaldehyde degradation technologies primarily include physical adsorption,[1] biological methods,[3] photo-oxidation,[4] and metal oxide oxidation.[5] Formaldehyde, owing to its reducing nature, can be readily degraded when oxidized by oxidizing agents. Catalytic oxidation methods exhibit high degradation efficiency and can achieve complete mineralization of formaldehyde. Therefore, catalytic oxidation is suitable for treating formaldehyde-containing wastewater at varying concentrations.[6-8]

Catalytic oxidation using hydrogen peroxide (H_2O_2) as the oxidizing agent demonstrates both environmental compatibility and high efficiency.[9] Due to its low cost and environmental friendliness, H_2O_2 is widely used in wastewater treatment. H_2O_2 shows high efficiency in degrading organic pollutants and does not produce byproducts other than water during the oxidation and decomposition process. Therefore, H_2O_2 is considered an ideal oxidizing agent for the oxidative treatment of organic pollutants. However, the oxidation ability of H_2O_2 alone is weak; it must be catalyzed by a catalyst to produce strong hydroxyl radicals (HO•) and other reactive species that react with organic compounds in wastewater, leading to their degradation.

The most widely used process in catalytic oxidation using H_2O_2 as the oxidizing agent is the Fenton oxidation process.[10-12] By activating H_2O_2 with Fe^{2+}, strong hydroxyl radicals are produced. However, in this process, large amounts of Fe^{2+} and acid are consumed, and iron sludge is generated.[13,14] To overcome these limitations of the Fenton process, it is necessary to explore alternative catalysts that are most cost-effective and energy-efficient. For example, Imohiosen *et al*.[15] synthesized a nanoscale zero-valent iron (nZVI) catalyst using plant leaf extract. The effectiveness of the H_2O_2-supported nZVI catalyst in treating pharmaceutical effluent was evaluated. The degradation efficiency of pharmaceutical effluent by H_2O_2 was improved using the prepared nZVIs. Moreover, the nZVIs were relatively stable and maintained their catalytic activity even after being recycled up to 5 times. However, the improvement was not significant, with a maximum degradation rate of only 81%.

Doping the rare earth metal lanthanum (La) into catalysts can improve their catalytic activity and adsorption performance.[16-19] To date, studies on La have mainly focused on its application in the photocatalytic treatment of wastewater.[20,21] The emergence of photocatalysis has provided an environmentally friendly alternative for removing organic contaminants from water. When the catalyst absorbs a sufficient amount of energy, reactive species are generated on its surface, which then participate in oxidation and reduction reactions. For example, La-based catalysts can catalyze molecular oxygen to produce superoxide radicals and water molecules to produce hydroxyl radicals.[22,23] Although photocatalytic reactions are environmentally friendly, they often suffer from long degradation times and low degradation efficiencies.

For example, Iqbal[17] synthesized a new type of La-doped zinc (Zn) oxide nanoparticles and investigated their degradation performance toward rhodamine B dye. The maximum degradation rate of rhodamine B dye was 84.97% after 150 min. The catalytic activity of La can be further enhanced by loading it onto different types of support materials. For example, Wang *et al*.[24] synthesized La/manganese (Mn)-doped titanium dioxide nanotube arrays (La/Mn-TNAs) using the anodic oxidation method. The degradation rate of organic dyes by the synthesized La/Mn-TNAs exceeded 90%. The doping of La and Mn into nanotube arrays had a significant effect on catalytic activity.

It is well known that zeolite Socony Mobil-5 (ZSM-5) is a common adsorbent that promotes the removal of pollutants from aqueous solution through adsorption facilitated by its unique porous structure.[25,26] Studies have revealed that loading La onto ZSM-5 is an effective method to enhance photocatalytic activity.

Bifunctional catalysts possessing both adsorption and catalytic activity have demonstrated promising potential in numerous catalytic processes.[27-29] La- and Zn-modified H-ZSM–5 zeolites generate highly reactive electrons and electron–hole pairs, thereby enhancing the catalytic activity and stability of H-ZSM–5. Under mercury lamp irradiation, the removal efficiency of phenol can reach 99.38% at 60℃ with La- and Zn-modified H-ZSM–5 as the catalyst and H_2O_2 as the oxidant.[30] However, this type of catalyst has not yet been utilized for formaldehyde removal in wastewater treatment. Therefore, improving catalyst preparation methods and optimizing the composition of active components in catalysts are necessary to enhance the formaldehyde removal efficiency in wastewater.

In this study, we successfully synthesized a La oxide (La_2O_3)–zeolite composite catalyst with dual functionality. During preparation, a La nitrate solution was first adsorbed into the porous framework and onto the surface of the zeolite. Subsequently, through high-temperature calcination, the La nitrate decomposed and transformed into active La_2O_3 species. After this treatment, La_2O_3 was uniformly dispersed on the outer surface and within the pores of the zeolite, forming highly dispersed active sites. This unique structure not only significantly increases the effective contact area between La_2O_3 and formaldehyde molecules but also enhances the stability of the active components, thereby achieving efficient catalytic degradation of formaldehyde under room-temperature conditions and

demonstrating excellent environmental purification performance.

2. Materials and methods

2.1. Materials

All reagents used in this study—including formaldehyde solution (37 wt%; Sinopharm Chemical Reagent Co., Ltd., China), H_2O_2 solution (30 wt%; Sinopharm Chemical Reagent Co., Ltd., China), La nitrate Sinopharm Chemical Reagent Co., Ltd., China), H-ZSM–5 (Sinopharm Chemical Reagent Co., Ltd., China), acetylacetone (Sinopharm Chemical Reagent Co., Ltd., China), glacial acetic acid (Sinopharm Chemical Reagent Co., Ltd., China), ammonium acetate (Sinopharm Chemical Reagent Co., Ltd., China), and tert-butanol (Sinopharm Chemical Reagent Co., Ltd., China)—were of analytical grade.

2.2. Preparation of La oxide/ZSM-5

A total of 0.560 g of La(III) nitrate hexahydrate ($La[NO_3]_3 \cdot 6H_2O$) was accurately weighed and placed in a clean beaker. Then, 4 mL of deionized water was added, and the mixture was stirred until the $La(NO_3)_3 \cdot 6H_2O$ was completely dissolved. Subsequently, 4 g of ZSM-5 was slowly added to the $La(NO_3)_3 \cdot 6H_2O$ solution, and the mixture was soaked for 4 h. The resulting mixture was then dried in an oven at 100°C for 2 h. After drying, the sample was transferred to a crucible and calcined in a muffle furnace at 700°C for 4 h. The resulting calcined product was referred to as La_2O_3/ZSM-5. The La_2O_3 loading accounted for 5% of the total mass of La_2O_3/ZSM-5. Samples with La_2O_3 mass fractions of 10%, 15%, 20%, and 25% were prepared using the same procedure.

2.3. Characterization of La oxide/ZSM-5

The thermal stability of undried ZSM-5, $La(NO_3)_3 \cdot 6H_2O$, and the dried ZSM-5/La_2O_3 mixture was evaluated using a thermogravimetric (TG) analyzer (Perkin Elmer, USA). The measurements were performed in air at a flow rate of 20 mL/min over a temperature range of 35–800℃ with a heating rate of 20℃/min. The crystal structures of ZSM-5 alone and ZSM-5 loaded with La_2O_3 at 5%, 10%, and 15% loading levels were analyzed using an X-ray powder diffractometer (XRD; Rigaku, Japan). The valence state of La on the surface of the ZSM-5 sample containing 10% La_2O_3 loading was determined by X-ray photoelectron spectroscopy (XPS; Thermo Fisher Scientific, USA). Transmission electron microscopy (TEM) coupled with energy-dispersive spectroscopy (JEOL, Japan) was employed to analyze the distribution of La within the ZSM-5 framework.

2.4. Formaldehyde degradation reaction

A 5 mL aliquot of formaldehyde standard solution was added to a 25 mL reaction tube. Under continuous stirring, an appropriate amount of La_2O_3/ZSM-5 was added to the solution. After thorough mixing of the suspension, 30% H_2O_2 was added at 25°C to initiate the formaldehyde degradation reaction. Samples were collected every 4 min, and after five sampling intervals, the reaction was stopped. Each withdrawn sample was transferred to a volumetric flask containing acetylacetone, diluted to the mark with deionized water, and derivatized in a water bath at 100℃ for 3 min. After cooling to room temperature, the absorbance was measured at 414 nm using deionized water as a blank. The formaldehyde degradation rate was then calculated.

2.5. Analytical method

Standard solutions of formaldehyde were prepared and calibrated using the iodometric titration technique. The calculation of the degradation rate of the standard formaldehyde solution used the acetylacetone colorimetric method. Formaldehyde reacts with acetylacetone to form a yellow-colored compound. The concentration of the resulting compound was determined by measuring its absorbance at 414 nm using a visible spectrophotometer (Shanghai Jinghua Technology Instrument Co., Ltd., China). The measured absorbance corresponded to the formaldehyde concentration. A standard calibration curve of formaldehyde concentration versus absorbance was plotted.[6]

3. Results and discussion

3.1. Standard curve for formaldehyde determination

As shown in Figure 1, the formaldehyde concentration range of 0.3–3.0 μg/mL exhibited excellent linearity with the absorbance of the formaldehyde–acetylacetone derivative. Based on this quantitative relationship, sample absorbance values were applied to the standard curve to determine the residual formaldehyde concentrations. The degradation rate was calculated by comparing these values with the initial formaldehyde concentration.

3.2. Determination of the calcination temperature of the La oxide/ZSM-5 precursor

The TG analysis curves of the La_2O_3/ZSM-5 precursor sample dried at 100°C, the undried ZSM-5 sample, and the $La(NO_3)_3 \cdot 6H_2O$ sample are shown in Figure 2. All samples exhibited weight loss below 250°C, which was likely due to the loss of adsorbed water and interlayer water.[31] In addition, two major thermal events were observed for $La(NO_3)_3 \cdot 6H_2O$: Between 487°C and 587°C, significant weight loss occurred due to its thermal decomposition, while further decomposition of residual $La(NO_3)_3$ between 587°C and 735°C produced La_2O_3.

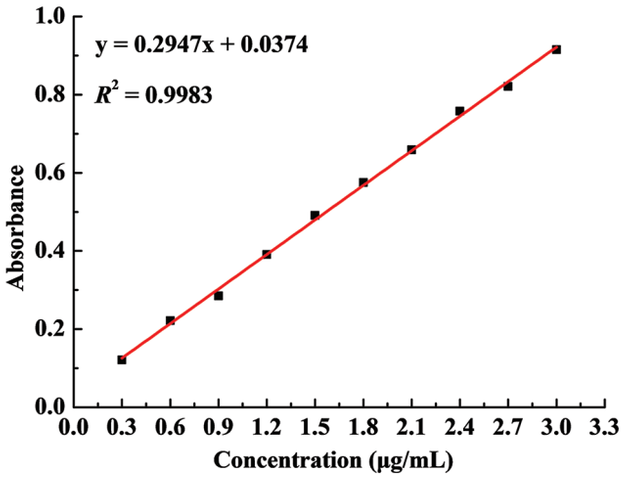

Figure 1. Standard curve of formaldehyde showing the relationship between the concentration and absorbance

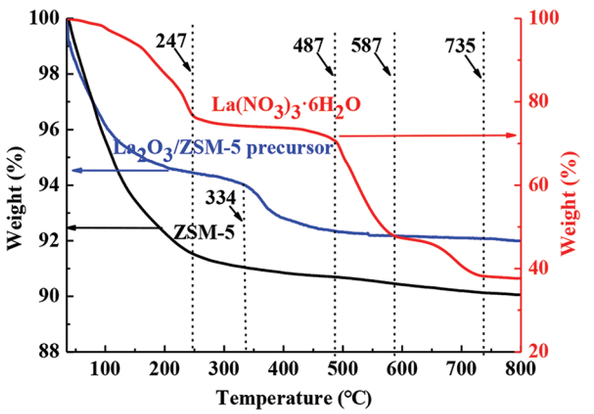

Figure 2. Thermogravimetric curves of La_2O_3/ZSM-5, ZSM-5, and $La(NO_3)_3 \cdot 6H_2O$

Abbreviations: La_2O_3: Lanthanum oxide; $La(NO_3)_3 \cdot 6H_2O$: Lanthanum(III) nitrate hexahydrate; ZSM-5: Zeolite Socony Mobil-5.

A decrease in the thermal stability of $La(NO_3)_3$ was observed when it was mixed with ZSM-5, which may be attributed to interactions between NO_3^- ions in $La(NO_3)_3$ and the acidic sites of ZSM-5. These interactions likely lower the activation energy required for decomposition, thereby reducing the thermal stability of $La(NO_3)_3$. Another possible explanation is that $La(NO_3)_3$ was dispersed on the ZSM-5 surface in a monolayer or near-monolayer form, leading to a decrease in its decomposition temperature. TG analysis revealed negligible weight loss above 700°C. Therefore, the optimal calcination temperature was determined to be 700°C.

3.3. X-ray powder diffraction characterization

As shown in Figure 3, the crystallization of ZSM-5 was consistent with the reported standard diffraction pattern, exhibiting the typical XRD pattern of ZSM-5 zeolite.[32] Although ZSM-5 exhibited numerous diffraction peaks, the strongest and most characteristic diffraction peaks were observed at 7.9°, 8.9°, 23.1°, 23.9°, and 24.4°. In general, higher crystallinity corresponds to stronger and sharper diffraction peaks.[33,34]

The diffraction peaks of La_2O_3 obtained after calcination of $La(NO_3)_3$ were located at 15.72°, 27.96°, 39.58°, 48.58°, 55.36°, 64.3°, and 69.84°, consistent with the reported standard diffraction pattern of La_2O_3 (JCPDS No. 02–0607).[35,36]

As shown in Figure 3, with increasing La_2O_3 loading, the characteristic XRD peak intensity of ZSM-5 gradually weakened. Notably, no distinct

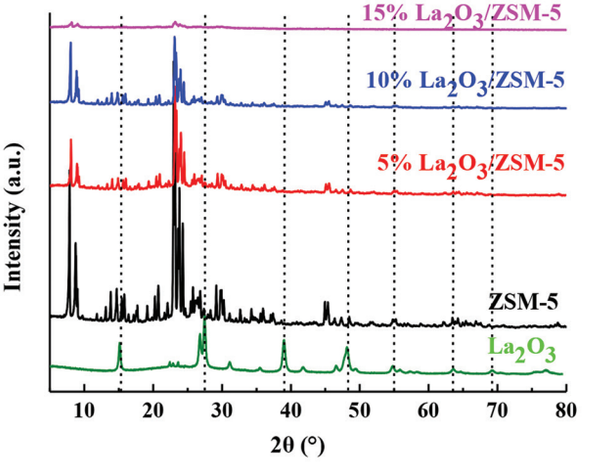

Figure 3. X-ray diffraction patterns of La_2O_3, ZSM-5, 5% La_2O_3/ZSM-5, 10% La_2O_3/ZSM-5, and 15% La_2O_3/ZSM-5

Abbreviations: La_2O_3: Lanthanum oxide; ZSM-5: Zeolite Socony Mobil-5.

independent diffraction peaks of La_2O_3 were observed in the diffraction pattern. This phenomenon may be attributed to the high dispersion of La_2O_3 on the surface or within the pores of the ZSM-5. Such a dispersed state prevents La_2O_3 from forming a significant crystalline structure, thereby suppressing the intensity of the original crystalline phase diffraction peaks of ZSM-5 and effectively masking the crystalline phase diffraction signals of La_2O_3, making them undetectable with clarity.

3.4. X-ray photoelectron spectroscopy characterization

Figure 4 displays the XPS spectrum of ZSM-5 loaded with 10% La_2O_3 after calcination at 700℃. Typical La $3d_{5/2}$ and La $3d_{3/2}$ spectra were observed, confirming the chemical state of La in ZSM-5. As shown in Figure 4, the La $3d_{5/2}$ peak appeared at 835.1 eV, with a corresponding satellite peak at 838.8 eV. The La $3d_{3/2}$ peak appeared at 851.9 eV, with a satellite peak at 855.6 eV. The energy difference between the La $3d_{3/2}$ and $3d_{5/2}$ states was approximately 16.8 eV, which is consistent with the characteristic values of La_2O_3.[36,37] Based on these results, La exists in the form of La_2O_3 in La_2O_3/ZSM-5.

3.5. TEM-energy dispersive spectroscopy analysis

Figure 5 presents the TEM image of the La_2O_3/ZSM-5 catalyst along with the corresponding elemental distribution maps. The maps clearly show that La was uniformly dispersed within the framework structure of ZSM-5, with no obvious regions of enrichment or agglomeration. This observation is consistent with the XRD results: No characteristic diffraction peaks of La_2O_3 were detected, further confirming that La species were successfully and uniformly introduced into the lattice structure of the ZSM-5. If any La_2O_3 crystals were formed, their crystallite size is extremely small and thus not detectable by XRD.

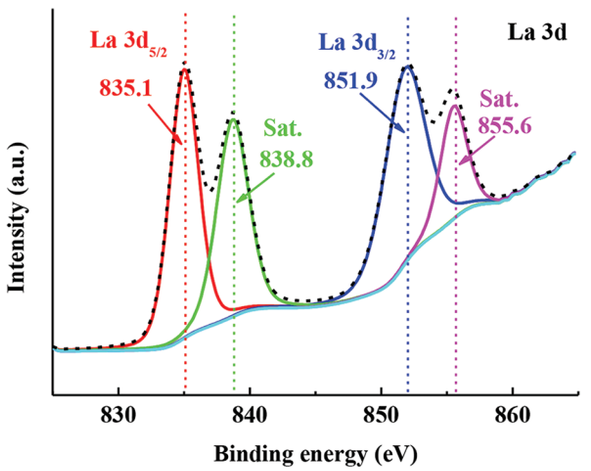

Figure 4. La 3d X-ray photoelectron spectra of La_2O_3/ZSM-5

Abbreviations: La: Lanthanum; La_2O_3: Lanthanum oxide; ZSM-5: Zeolite Socony Mobil-5.

3.6. Factors influencing formaldehyde degradation

The effect of La_2O_3 loading in La_2O_3/ZSM-5 (5%, 10%, 15%, 20%, and 25%) on formaldehyde degradation rates was investigated. Hydrogen peroxide (43 μL) was added to a formaldehyde solution (5 mL), then added La_2O_3/ZSM-5 with La_2O_3 loadings of 5%, 10%, 15%, 20%, and 25% respectively, and reacted at 25°C for 20 min. These findings indicate that when the loading amount of La_2O_3 on La_2O_3/ZSM-5 was below 15%, the formaldehyde degradation rate increased with the increase in La_2O_3 loading. However, when the loading amount exceeded 15%, further increases in La_2O_3 loading resulted in only marginal improvement in the formaldehyde degradation rate. The high dispersion of La_2O_3 on ZSM-5 may have influenced the formaldehyde degradation efficiency.

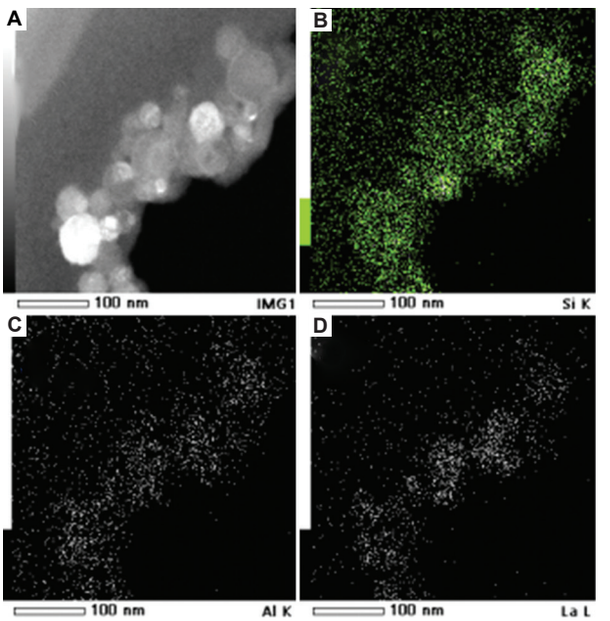

Figure 5. Transmission electron micrography images of La_2O_3/ZSM-5: (A) general morphology and (B-D) elemental mapping of La_2O_3/ZSM-5 in the presence of (B) Si, (C) Al, (D) and La (scale bar: 100 nm; magnification: ×50,000)

Abbreviations: Al: Aluminum; La: Lanthanum; La_2O_3: Lanthanum oxide; Si: Silicon; ZSM-5: Zeolite Socony Mobil-5.

Given that the formaldehyde degradation rate of La_2O_3/ZSM-5 loaded with 15% La_2O_3 (93.5%) showed only a slight increase compared with that loaded with 10% La_2O_3 (92.7%), and considering the need to minimize the use of the relatively expensive rare earth element La, subsequent experiments utilized La_2O_3/ZSM-5 catalysts with a La_2O_3 loading of 10%.

The effect of the La_2O_3/ZSM-5 dosage on formaldehyde degradation efficiency was investigated under reaction conditions of 25℃, 43 μL H_2O_2, and 20 min. As shown in Figure 6, the formaldehyde degradation efficiency increased with the amount of La_2O_3/ZSM-5. Previous research has also reported that in formaldehyde degradation experiments using La_2O_3/ZSM-5 catalysts, when the dosage was set at 60 mg/mL and 70 mg/mL, respectively, the degradation efficiency of formaldehyde reached 100% after a reaction time of 20 min. However, the highest degradation rate was observed at 70 mg/mL La_2O_3/ZSM-5, where 100% degradation was achieved within 16 min. This result indicates that within a specific concentration range, the catalyst exhibits high efficiency in removing formaldehyde and can achieve complete degradation in a relatively short period of time. By increasing the amount of La_2O_3/ZSM-5, the total surface area of the catalyst is significantly enhanced, along with the number of active sites. This change directly increases the probability of effective interaction between active formaldehyde or H_2O_2 molecules and the catalyst surface, thereby facilitating the catalytic reaction.[7,38]

To further determine the activation capacity of La_2O_3/ZSM-5 toward H_2O_2, the effect of H_2O_2 dosage on the formaldehyde degradation rate was investigated under reaction conditions of 25℃, 50 mg/mL La_2O_3/ZSM-5, and a reaction time of 20 min. As shown in Figure 7, as the amount of H_2O_2 increased, the degradation rate of formaldehyde also increased. However, when the molar ratio of H_2O_2 to formaldehyde exceeded 3, further increases in H_2O_2 dosage had a limited effect on enhancing the reaction rate and degradation efficiency. This is because, without increasing the dosage of La_2O_3/ZSM-5, simply adding more H_2O_2 cannot significantly increase the number of active oxygen species in the reaction system, and the number of formaldehyde molecules available for activation is also limited.

Under reaction conditions of 25℃, 50 mg/mL La_2O_3/ZSM-5, a molar ratio of H_2O_2 to formaldehyde of 3, and a reaction time of 20 min, the effect of formaldehyde concentration on the degradation reaction was investigated by varying the formaldehyde concentration (0.25 mg/mL, 0.499 mg/mL, 0.998 mg/mL, 1.497 mg/mL, and 1.996 mg/mL). The experimental results are shown in Figure 8. The findings indicate that when the formaldehyde concentration is below 1.497 mg/mL, the degradation efficiency of formaldehyde can reach over 91%. Furthermore, previous studies have shown that within this concentration range, as the initial formaldehyde concentration gradually increases, its degradation rate tends to decrease.

Under reaction conditions of 25℃, 50 mg/mL La_2O_3/ZSM-5, a molar ratio of H_2O_2 to formaldehyde of 3, and a reaction time of 20 min, the formaldehyde degradation rates under different pH values—pH 1, 3, 5, 7, 9, 11, and 13—were found to be 85.6%, 88.1%, 98.4%, 100%, 100%, 95.0%, and 84.7%, respectively.

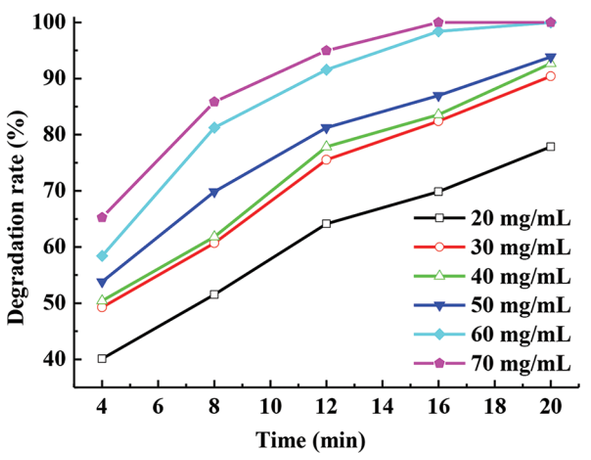

Figure 6. Effect of lanthanum oxide/Zeolite Socony Mobil-5 dosage on the formaldehyde degradation efficiency

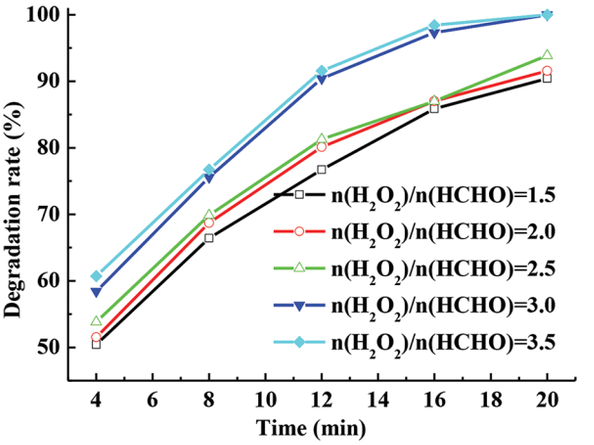

Figure 7. Effect of the H_2O_2-to-HCHO molar ratio on the HCHO degradation rate

Abbreviations: H_2O_2: Hydrogen peroxide; HCHO: Formaldehyde.

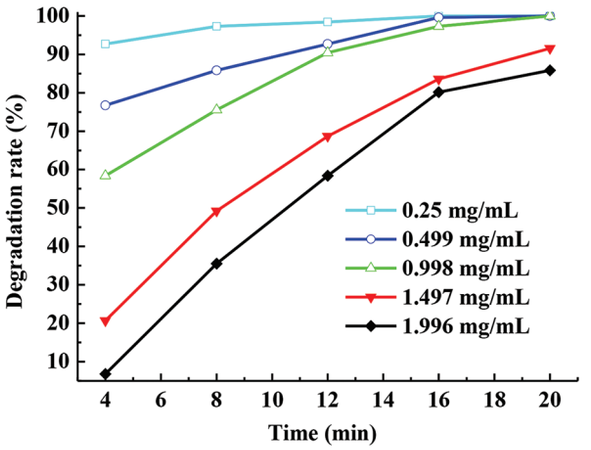

Figure 8. Effect of formaldehyde concentration on its degradation rate

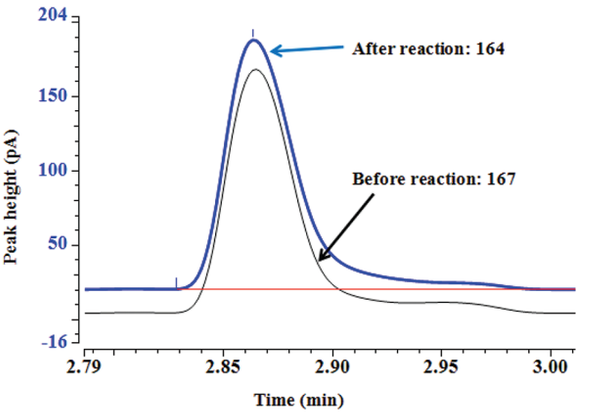

Figure 9. Gas chromatographic analysis of tert-butanol

This finding indicates that the degradation performance under neutral conditions is superior to that under acidic and alkaline conditions. The degradation efficiency decreased significantly under highly acidic or alkaline conditions. A highly acidic environment may disrupt the structure of the catalyst, whereas a highly alkaline environment may suppress hydroxyl group formation.

In this study, tert-butanol was employed as a radical scavenger as it readily reacts with hydroxyl radicals. Hydroxyl radicals react with tert-butanol primarily through hydrogen atom elimination from carbon, producing a tert-butoxy radical. The tert-butoxy radical then rapidly undergoes β-scission, yielding acetone and a methyl radical.[39] On the addition of tert-butanol, the formaldehyde degradation rate decreased significantly, from 100% to 32%, confirming the participation of hydroxyl radicals in the reaction.

To further verify hydroxyl radical generation during the formaldehyde catalytic degradation over La_2O_3/ZSM-5, a supplementary gas chromatographic analysis was performed. A mixture containing 1 mL tert-butanol, 0.25 g La_2O_3/ZSM-5, and 50 µL H_2O_2 was allowed to react for 20 min. Samples (5 µL each) collected before and after the reaction were diluted in 10 mL dioxane and analyzed by gas chromatography (injection port temperature: 150 ℃; detector temperature: 180℃; column temperature: 50–110℃; heating rate: 5℃/min). As shown in Figure 9, the results indicated no significant change in tert-butanol content and no new peaks corresponding to reaction byproducts, thereby confirming that hydroxyl radicals were not involved in the degradation process.

To investigate the mechanism of La2O3/ZSM-5 on hydrogen peroxide, the catalyst, La_2O_3/ZSM-5, was added to an H_2O_2 solution and allowed to react for 20 min. The concentration of H_2O_2 decreased by only 0.2 mol/L before and after the reaction, indicating that La_2O_3/ZSM-5 catalyzes the decomposition of H_2O_2 or the generation of free radicals at a relatively slow rate.

To further evaluate the catalytic contribution of La_2O_3/ZSM-5, adsorption and oxidation experiments were conducted under comparable conditions. In the formaldehyde adsorption tests performed using La_2O_3/ZSM-5 and ZSM-5 separately, adsorption rates of 23.07% and 20.5% were obtained, respectively, by adding 0.25 g of La_2O_3/ZSM-5 and ZSM-5, respectively, to 5 mL of formaldehyde solution and stirring at 25℃ for 20 min without H_2O_2. In contrast, H_2O_2 oxidation of formaldehyde in the absence of La_2O_3/ZSM-5 (5 mL formaldehyde solution, 50 µL H_2O_2, no catalyst, 25℃, 20 min) resulted in a degradation rate of only 36.5%. This finding indicates that La_2O_3/ZSM-5 exhibits a significant catalytic activation effect in the reaction system.

According to the kinetic study by Mandal *et al.*,[40] an unusual oxidation state of La (La^{4+}) was observed during the interaction between H_2O_2, La_2O_3, and formaldehyde. The addition of tert-butanol significantly reduced the oxidation reaction of formaldehyde, possibly by inhibiting the interaction between the catalyst and H_2O_2 or between the catalyst and formaldehyde. This finding indicates that the oxidation reaction of formaldehyde catalyzed by La_2O_3/ZSM-5 is not purely radical.[5] La_2O_3/ZSM-5 demonstrates multiple functions, including adsorption and activation of formaldehyde molecules and H_2O_2 molecules.

After three recycling cycles, the formaldehyde degradation rate of La_2O_3/ZSM-5 decreased from 100% to 91.5%, while the conversion efficiency dropped by

8.5%. Inductively coupled plasma–optical emission spectrometry analysis revealed that the La content in the La_2O_3/ZSM-5 decreased by 1.9% after three reaction cycles. Although the reusability and stability of the catalyst are of great significance for reducing catalyst costs, the findings of this study indicate that the stability and activity of the catalyst in solution are not yet ideal. For example, in formaldehyde degradation catalysis, a magnesium oxide/γ-aluminum oxide catalyst exhibited a degradation rate decrease from 99.85% to 87.53% after six cycles of use[5]; whereas the MIL-100(Fe) catalyst showed a decrease from 91.7% to 65.9% after five cycles of use.[41] Therefore, future research should focus on improving both the activity and stability of catalysts.

4. Conclusion

A La_2O_3/ZSM-5 catalyst with high catalytic activity was produced using the equal-volume impregnation method. XPS testing confirmed the formation of La_2O_3, while XRD and TEM analyses verified its high dispersion on the ZSM-5 support. This catalyst possesses multiple functions, including the adsorption and activation of formaldehyde molecules and H_2O_2 molecules. The catalytic efficiency was shown to depend strongly on experimental conditions such as catalyst concentration, H_2O_2 concentration, pH, reaction time, and formaldehyde concentration. Under reaction conditions of 25℃, 50 mg/mL La_2O_3/ZSM-5, 50 μL H_2O_2, pH 5–11, and a reaction time of 20 min, the formaldehyde degradation rate exceeded 95%. The La_2O_3/ZSM-5 catalyst demonstrates stability under both acidic and alkaline conditions. Even at a formaldehyde concentration of 1.497 mg/mL, the degradation rate remained at 91%. This method demonstrates great potential for practical applications in formaldehyde degradation processes.

Acknowledgments

None.

Funding

This study was supported by the National Natural Science Fund of China (grant no. 22072105).

Conflict of interest

The authors declare they have no competing interests.

Author contributions

Conceptualization: Qingguo Ma, Ye Yuan
Formal analysis: Qingguo Ma, Ye Yuan
Investigation: Sai Yuan, Ye Yuan, Jun Zhong, Ran Wang, Yujie Gong, Qin Gao
Methodology: Qingguo *Ma,* Sai Yuan, Ye Yuan
Writing–original draft: Sai Yuan, Ye Yuan
Writing–review & editing: Qingguo Ma

Availability of data

Data is available from the corresponding author upon reasonable request.

References

1. Yang X, Zhao HQ, Qu ZB, *et al*. The effect of oxygen-containing functional groups on formaldehyde adsorption in solution on carbon surface: A density functional theory study. *J Environ Chem Eng*. 2021;9(5):105987. doi: 10.1016/j.jece.2021.105987
2. Guimaraes JR, Farah CRT, Maniero MG, Fadini PS. Degradation of formaldehyde by advanced oxidation processes. *J Environ Manage*. 2012;107:96-101. doi: 10.1016/j.jenvman.2012.04.024
3. Lebkowska M, Narozniak-Rutkowska A, Pajor E. Effect of a static magnetic field of 7 mT on formaldehyde biodegradation in industrial wastewater from urea-formaldehyde resin production by activated sludge. *Bioresour Technol*. 2013;132:78-83. doi: 10.1016/j.biortech.2013.01.020
4. Laciste MT, De Luna MDG, Tolosa NC, Lu MC. Effect of calcination time of a quadruple-element doped titania nanoparticles in the photodegradation of gaseous formaldehyde under blue light irradiation. *Chemosphere*. 2020;246:125763. doi: 10.1016/j.chemosphere.2019.125763
5. Du L, Li PY, Gao WQ, Ding X, Jiao WZ, Liu YZ. Enhancement degradation of formaldehyde by MgO/γ-Al_2O_3 catalyzed O_3/H_2O_2 in a rotating packed bed. *J Taiwan Inst Chem E*. 2021;118:29-37. doi: 10.1016/j.jtice.2021.01.011
6. Ma QG, Huo PC, Wang KS, *et al*. Preparation of perovskite-type $LaMnO_3$ and its catalytic degradation of formaldehyde in wastewater. *Molecules*. 2024;29(16):3822. doi: 10.3390/molecules29163822
7. Ma QG, Shi SY, Yang FF, Zhang X. Removal of formaldehyde in water with low concentration of hydrogen peroxide catalyzed by lanthanumsilicon oxide composite. *Desalin Water Treat*. 2023;300:101-106. doi: 10.5004/dwt.2023.29734

8. Ma QG, Hao Y, Xue YF, Niu YL, Chang XL. Removal of formaldehyde from aqueous solution by hydrogen peroxide. *J Water Chem Techno.* 2022;44(4):297-303. doi: 10.3103/S1063455X22040099
9. Zhang XC, Cheng SL, Liao FT, Chen C, Long MC. Research progress on hydrogen peroxide photosynthesis from only water and oxygen over polymer photocatalysts. *Rare Metals*. 2024;43(12):6144-6163. doi: 10.1007/s12598-024-02752-3
10. Bahammou O, Tazi I, El Mrabet I, *et al*. Treatment of real tannery industrial wastewater via sequential biological and US/UV/activated persulfate-hydrogen peroxide processes. *Water Air Soil Pollut*. 2025;236(5):282. doi: 10.1007/s11270-025-07904-4
11. El Mrabet I, Benzina M, Valdes H, Zaitan H. Treatment of landfill leachates from Fez city (Morocco) using a sequence of aerobic and Fenton processes. *Sci Afr*. 2020;8:e00434. doi: 10.1016/j.sciaf.2020.e00434
12. Chen JP, Peng YA, Wang ZK, Lv FG. Influence of Fentonlike reactions between hydrogen peroxide and ferric chloride on chemical mechanical polishing 304 stainless steel. *Int J Adv Manuf Tech*. 2024;131:2667-2675. doi: 10.1007/s00170-023-12117-2
13. Sani S, Dashti AF, Adnan R. Applications of Fenton oxidation processes for decontamination of palm oil mill effluent: A review. *Arab J Chem*. 2020;13(10):7302-7323. doi: 10.1016/j.arabjc.2020.08.009
14. Oluwole AO, Omotola EO, Olatunji OS. Pharmaceuticals and personal care products in water and wastewater: A review of treatment processes and use of photocatalyst immobilized on functionalized carbon in AOP degradation. *BMC Chem*. 2020;14(1):62. doi: 10.1186/s13065-020-00714-1
15. Imohiosen FA, Ofudje EA, Al-Ahmary KM, *et al*. Pharmaceutical effluent degradation using hydrogen peroxide-supported zerovalent iron nanoparticles catalyst. *Sci Rep.* 2024;14(1):23957. doi: 10.1038/s41598-024-74627-7
16. Prabagar JS, Yashas SR, Gurupadayya B, Wantala, K, Diganta D, Shivaraju HP. Degradation of doxycycline antibiotics using lanthanum copper oxide microspheres under simulated sunlight. *Environ Sci Pollut R*. 2022;29(38):57204-57214. doi: 10.1007/s11356-022-19842-3
17. Iqbal T, Sohaib M. Synthesis of novel lanthanum-doped zinc oxide nanoparticles and their application for wastewater treatment. *Appl Nanosci*. 2021;11(10):2599-2609. doi: 10.1007/s13204-021-02104-y
18. Teju MD, Majamo SL. Synthesis and application of lanthanum-doped magnetic biochar composite adsorbent for removal of fluoride from water. *Environ Monit Assess*. 2023;195(12):1469. doi: 10.1007/s10661-023-12075-y
19. Kumari A, Kumar A, Thakur M, Pathania D, Rani A, Sharma A. Murraya koenigii plant-derived biochar (BC) and lanthanum ferrite (BC/$LaFeO_3$) nano-hybrid structure for efficient ciprofloxacin adsorption from waste water. *Chem Afr*. 2023;6:3079-3095. doi: 10.1007/s42250-023-00698-0
20. Chakraborty V, Das P, Roy PK. Lanthanum oxide-graphene oxide coated functionalized pyrolyzed biomass from sawdust and its application for dye removal present in solution. *Biomass Convers Bior*. 2023;13(7):5601-5610. doi: 10.1007/s13399-021-01507-9
21. Heydari R, Akhlaghian F. Promotion of brass nanowires with lanthanum oxide and its application for photodegradation of tetracycline wastewater. *Environ Sci Pollut R*. 2021;28(8):9255-9266. doi: 10.1007/s11356-020-11450-3
22. Saien J, Soleymani AR. Feasibility of using a slurry falling film photo-reactor for individual and hybridized AOPs. *J Ind Eng Chem*. 2012;18(5):1683-1688. doi: 10.1016/j.jiec.2012.03.014
23. Mallikarjunaswamy C, Soundarya TL, Al-Kahtani AA, Al-Odayni AB, Nagaraju G, Ranganatha VL. Facile green synthesis of lanthanum oxide nanoparticles: Their photocatalytic and electrochemical applications. *J Mater Sci Mater Electron*. 2024;35(18):1203. doi: 10.1007/s10854-024-13024-2
24. Wang WX, Zhang JB, Liang DX, *et al*. Anodic oxidation growth of lanthanum/manganese-doped TiO_2 nanotube arrays for photocatalytic degradation of various organic dyes. *J Mater Sci Mater El*. 2020;31(11):8844-8851. doi: 10.1007/s10854-020-03419-2
25. Liao J, Bao W, Chen Y, Zhang Y, Chang L. The adsorptive removal of thiophene from benzene over ZSM-5 Zeolite. *Energ Source Part A*. 2012;34(5-8):618-625. doi: 10.1080/15567036.2010.549916
26. Ren XC, Wang ZK, Zhang GX. Mechanism of NO adsorption on H-ZSM-5 under aerobic atmosphere. *J Wuhan Univ Technol-Mater Sci Ed*. 2025;40(3):674-681. doi: 10.1007/s11595-025-3103-y
27. Li N, Huang B, Dong X, *et al*. Bifunctional zeolites-silver catalyst enabled tandem oxidation of formaldehyde at low temperatures. *Nat Commun*. 2022;13(1):2209. doi: 10.1038/s41467-022-29936-8
28. Tang XF, Li YG, Huang XM, *et al*. MnO_x-CeO_2 mixed oxide catalysts for complete oxidation of formaldehyde: Effect of preparation method and calcination temperature. *Appl Catal B Environ*. 2006;62(3-4):265-273. doi: 10.1016/j.apcatb.2005.08.004
29. Chen D, Qu ZP, Sun YH, Gao K, Wang Y. Identification of reaction intermediates and mechanism responsible for highly active HCHO oxidation on Ag/MCM-41 catalysts. *Appl Catal B Environ*. 2013;142:838-848. doi: 10.1016/j.apcatb.2013.06.025
30. Song XL, Fu YX, Pang YM, Gao LG. Preparation of La-Zn/HZSM-5 zeolite and its application in

photocatalytic degradation of phenol. *Chem Phys Lett*. 2022;805:139947.
doi: 10.1016/j.cplett.2022.139947

31. Hellal MS, Rashad AM, Kadimpati KK, Attia SK, Fawzy ME. Adsorption characteristics of nickel (II) from aqueous solutions by zeolite scony mobile-5 (ZSM-5) incorporated in sodium alginate beads. *Sci Rep.* 2023;13(1):19601.
doi: 10.1038/s41598-023-45901-x
32. Ma YY, Hu J, Jia LH, Li ZF, Kan QB, Wu SJ. Synthesis, characterization and catalytic activity of a novel mesoporous ZSM-5 zeolite. *Mater Res Bull*. 2013;48:1881-1884.
doi: 10.1016/j.materresbull.2013.01.014
33. Li GX, Lei PJ, Chen G, *et al*. The effect of precursor temperature on the surface and interface structure of Ni/ZSM-5 hydrogenation catalyst. *Catal Lett*. 2025;155(5):163.
doi: 10.1007/s10562-025-05004-w
34. Zheng MD, Chen Y, Liu Z, *et al*. Hierarchically macroporous zeolite ZSM-5 microspheres for efficient catalysis. *Chem Res Chinese U*. 2024;40(4): 704-711.
doi: 10.1007/s40242-024-4041-5
35. Qi YC, Peng H. One-pot synthesis of La_2O_3-decorated Mg-Al oxides nanosheets for solar-light driven photocatalytic activity. *Colloid Surface A*. 2020;604:125316.
doi: 10.1016/j.colsurfa.2020.125316
36. Piskula ZS, Stodolny M, Gabala E, Kirszensztejn P, Nowicki W. Application of SiO_2-La_2O_3 amorphous mesoporous nanocomposites obtained by modified solegel method in high temperature catalytic reactions. *J Alloy Compd*. 2020;840:155635.
doi: 10.1016/j.jallcom.2020.155635
37. Fida H, Zhang G, Guo S, Naeem A. Heterogeneous fenton degradation of organic dyes in batch and fixed bed using La-Fe montmorillonite as catalyst. *J Colloid Interf Sci*. 2017;490:859-868.
doi: 10.1016/j.jcis.2016.11.085
38. Moothedan M, Sherly KB. Synthesis and characterization of nanomesoporous lanthanum aluminate ($LaAlO_3$) for catalytic wet air oxidation of phenol. *Emergent Mater*. 2020;3:267-277.
doi: 10.1007/s42247-020-00097-y
39. Flyunt R, Leitzke A, Mark G, *et al*. Determination of $^{\bullet}OH$, $O_2^{\bullet-}$, and hydroperoxide yields in ozone reactions in aqueous solution. *J Phys Chem B*. 2003;107(30):7242-7253.
doi: 10.1021/jp022455b
40. Mandal M, Chakraborty D. Kinetic investigation on the highly efficient and selective oxidation of sulfides to sulfoxides and sulfones with t-BuOOH catalyzed by La_2O_3. *RSC Adv*. 2015;5(16):12111.
doi: 10.1039/c4ra14391d
41. Mohammadifard Z, Saboori R, Mirbagheri NS, Sabbaghi S. Heterogeneous photo-Fenton degradation of formaldehyde using MIL-100(Fe) under visible light irradiation. *Environ Pollut*. 2019;251:783-791.
doi: 10.1016/j.envpol.2019.04.143